Repurposing the aldose reductase inhibitor and diabetic neuropathy drug epalrestat for the congenital disorder of glycosylation PMM2-CDG

Sangeetha Iyer[1], Kausalya Murthy[1], Zachary Parton[1], Hillary Tsang[1] Feba S. Sam[1], Nina DiPrimio[1], Jessica Lao[1] and Ethan O. Perlstein[1]

[1] Perlara PBC, 2625 Alcatraz Ave #435, Berkeley, California USA

Abstract

Phosphomannomutase 2 deficiency, or PMM2-CDG, is the most common congenital disorder of glycosylation affecting over 1,000 patients globally. PMM2 encodes an ancient metabolic enzyme that forms an obligate dimer that catalyzes an initial step in the conserved pathway leading to *N*-linked glycosylation of proteins in every cell of every animal throughout its life. All PMM2-CDG patients have at least some residual PMM2 enzymatic activity because complete loss of function is incompatible with life in humans as well as in yeast, flies, fish and mice. Here we describe the first nematode model of PMM2-CDG genetically engineered with the common F119L dimerization-defective patient allele, which has reduced PMM2 enzymatic activity, a constitutively activated ER stress response and an increased sensitivity to proteasome inhibition by bortezomib. We describe an unbiased phenotypic screen to identify FDA approved drugs and generally recognized as safe natural products that suppress bortezomib toxicity in PMM2 F119L homozygote mutant worms. Nine worm repurposing hits from this study and three yeast repurposing hits from a previous study were tested for their effect on PMM2 enzymatic activity in F119/R141H patient fibroblasts in a 96-well-plate assay. The yeast hit alpha-cyano-hydroxycinnamic acid (CHCA) and the worm hit pyrogallin rescue PMM2 enzymatic activity by 65.5% and 23% in PMM2 fibroblasts, respectively. CHCA shares the carboxylic acid-containing pharmacophore of aldose reductase inhibitors. We tested commercially available ARIs in worms and fibroblasts and we found that only epalrestat reproducibly rescues PMM2 enzymatic activity in both species. Epalrestat elevated PMM2 enzymatic activity in patient fibroblasts by 30% over baseline. Epalrestat reduced ER stress marker expression and increased PMM2 mRNA levels in PMM2 F119L homozygote mutant worms by a mechanism that appears to involve the transcriptional regulator NRF2. Epalrestat is the only safe, orally bioavailable and brain penetrant aldose reductase inhibitor approved for use in humans, and the first small molecule potentiator of PMM2 enzymatic activity.

Keywords: Phosphomannomutase 2 deficiency, drug repurposing, PMM2-CDG, congenital disorder of glycosylation, aldose reductase inhibitor, epalrestat

Introduction

Deficiency of the enzyme phosphomannomutase-2 caused by loss-of-function mutations in the human *PMM2* gene was shown over two decades ago to be the basis of a recessive congenital disorder of glycosylation originally called CDG1 or CDG1a. The first clinical observation by Jaeken and colleagues of a “carbohydrate-deficient glycoprotein syndrome” occurred four decades ago (Jaeken et al, 1980). The researcher and patient communities now refer to the disease as PMM2-CDG, the most common congenital disorder of glycosylation affecting at least 1,000 patients worldwide (Chang et al, 2018). Classical pediatric clinical presentations include developmental delay, severe encephalopathy with axial hypotonia, abnormal eye movements, psychomotor retardation and cerebellar hypoplasia (Matthijs et al, 1997). As patients reach their teenage years and young adulthood, health challenges include hypogonadism, coagulation abnormalities and thrombotic events, retinitis pigmentosa and peripheral neuropathy (Monin et al, 2014) The prognosis for PMM2-CDG patients is poor and there is currently no FDA approved treatment that targets the root cause of disease, namely PMM2 enzyme deficiency.

The PMM2 enzyme forms an obligate dimer in the cytoplasm that converts mannose-6-phosphate to mannose-1-phosphate, an initial essential step in the *N*-linked glycosylation of proteins. *N*-linked protein glycosylation is an evolutionarily conserved process that occurs in all animal cells throughout development and adulthood (Chang et al, 2018). PMM2-CDG is a multi-system, multi-organ disease because a minimal level of glycosylation is required at all times in all cells of the body, with cell types or organs more or less vulnerable to the complex sequelae of hypoglycosylation. For example, patients homozygous for a mutation in the promoter of PMM2 do not get PMM2-CDG or even a mild form of PMM2-CDG but instead have hyperinsulinemic hypoglycemia and polycystic kidney disease because this mutation impairs binding by a kidney- and pancreas-specific transcription factor to a chromatin loop in the promoter of PMM2 (Cabezas et al, 2017). As another example, hypoglycosylation of the calcium channel CACNA1A caused a gain-of-function channelopathy that in turn leads to an increase in stroke-like events in PMM2-CDG patients (Izquierdo-Serra et al, 2018).

Complete loss of *N*-linked protein glycosylation uniformly results in lethality of all animals in which PMM2 has been genetically knocked out, including humans. Homozygotes of the most common disease mutation, R141H, which is catalytically dead, have never been observed alive

in spite of the statistical predictions of population genetics (Matthijs et al, 1998; Kjaergaard et al, 1998). Those results indicate that there's a lower bound of PMM2 enzymatic activity (3-7%) required for viability but the minimal PMM2 enzymatic activity above which disease is suppressed is not known. Human genetics proves that this safety threshold varies from tissue to tissue, and it suggests that there are sharp tissue-specific transitions from physiology to pathophysiology with buffering capacity determined by both common and rare genetic modifiers in glycosylation and biologically related pathways (Citro et al, 2019).

Over 80% of disease-causing PMM2 alleles are missense mutations, resulting in amino-acid substitutions. Missense mutations fall into at least three biochemical classes: (i) protein destabilizing/misfolding mutations randomly distributed throughout the protein, (ii) dimerization defective mutations located in the monomer-monomer interface, and (iii) "catalytic dead" mutations in the active site (Yuste-Checa et al, 2015). Each PMM2 monomer forms a dimer with itself as a prerequisite for catalytic activity, though there need only be one functional active site per dimer (Andreotti et al, 2015). A plurality of PMM2-CDG patients across populations share the compound heterozygous genotype R141H/F119L, which pairs the aforementioned R141H null allele with the F119L dimerization-defective allele. Typically, patients present with R141H in compound heterozygosity with a hypomorphic mutation, often a rare or private mutation. Citro and colleagues argue that the tolerance of PMM2 to missense mutations compared to every other CDG gene suggests a fitness advantage to being a PMM2 carrier. As PMM2 enzymatic activity dips below 50%, at which point disease symptoms arise and how severely they arise are unknown because of the contribution of genetic modifiers that buffer the safety thresholds between health and disease. Similarly, it's unknown how small an increase in PMM2 enzymatic activity above disease baseline is required to elicit a therapeutic effect in PMM2-CDG patients.

A challenge for the PMM2-CDG community has been the inviability of mouse models and the lack of a gold standard cellular disease model given the fact that *N*-linked protein glycosylation is a process that occurs in all cell types throughout life. A morpholino-knockdown model of PMM2-CDG in zebrafish displayed what appeared to be disease relevant phenotypes but these results have not been confirmed in a genetic knockout mutant (Cline et al, 2012). Fly models of PMM2-CDG were generated and also exhibited what appeared to be disease relevant phenotypes but they suffer from early larval lethality, which is a difficult phenotype to rescue in a

genetic or chemical screen (Parkinson et al, 2016). For those reasons, we developed the first yeast models of PMM2-CDG (Lao et al, 2019).

We established evolutionarily conserved genotype-phenotype relationships across yeast and human patients between five PMM2 disease-causing mutations and their orthologous mutations in yeast. Overexpression of PMM2 in yeast cells lacking SEC53 (the yeast ortholog of PMM2) rescued lethality by mass action effects, and that there was no toxicity associated with overexpression of either PMM2 or SEC53 in yeast (Lao et al, 2019). Modest increases in SEC53 enzymatic activity translated into large phenotypic gains in yeast cell fitness. If the transition from physiology to pathophysiology is steep, is the transition from pathophysiology back to physiology equally steep? And are these sharp transitions conserved from yeast to humans? If the slopes of those transitions are conserved, small molecules are an attractive therapeutic modality not only because activation of PMM2 enzymatic activity appears to be well-tolerated but also because modest boosts in PMM2 enzymatic activity may be sufficient to produce real world clinical outcomes and disease modification.

A previous drug discovery effort for PMM2-CDG involved expression of recombinant human PMM2 protein in bacteria, a primary target-based differential scanning fluorimetry screen, and a secondary fibroblast-based PMM2 enzymatic activity assay in order to identify pharmacological chaperones (Yuste-Checa et al, 2017). Although this approach proved the concept that it is possible to discover pharmacological chaperones that increase PMM2 enzymatic activity, only one early-stage tool compound was identified and it is far from clinical candidacy. In order to address the urgent unmet medical needs of the PMM2-CDG community, we generated and characterized the first worm patient avatar of PMM2-CDG as a translational model between our previously published yeast models (Lao et al, 2019) and well-established PMM2-CDG patient fibroblasts. We created a F119L homozygous mutant worm for use in drug repurposing screens. We reasoned that worms would validate results from yeast, ensuring that the phenomena we observe a single-celled organism are conserved in a multicellular organism. We adapted a low-throughput PMM2 enzymatic activity assay to a multi-well-plate assay using patient fibroblasts (Van Schaftingen & Jaeken, 1995) in order to determine which hit compounds from yeast and worm drug repurposing screens also increase PMM2 enzymatic activity in human cells. Unexpectedly, we found that epalrestat, a generic diabetic peripheral neuropathy drug and the only safe aldose reductase inhibitor approved for use in humans (Hotta et al, 2006), is a

first-in-class PMM2 enzyme potentiator. We propose a mechanism of action that appears to involve an increase in PMM2 expression levels by the actions of the cytoprotective transcriptional regulator Nrf2 as well as an increase in the production of endogenous PMM2 coactivators that appears to involve inhibition of the polyol pathway.

Materials and Methods

Strains, cell lines and compounds

The pmm-2 mutant VC3054 was obtained from the Caenorhabditis Genetics Center (CGC). It's a homozygous lethal deletion chromosome balanced by GFP-marked translocation. COP1626 is the pmm-2 F125L (F119L in humans) hypomorphic homozygous mutant that was generated using CRISPR/Cas9 by NemaMetrix, Inc. The R141H/F119L patient fibroblast line GM20942 was obtained from Coriell. Screening was conducted using the 2,560-compound Microsource Spectrum library consisting of FDA approved drugs, bioactive tool compounds, and natural products. For all retests, compounds were reordered from Spectrum Discovery as 5 milligram dry powder stocks. (Note that the vendor has since gone out of business). Compounds were solubilized with fresh dimethylsulfoxide (DMSO) at high concentrations of 100mM or 50mM and stored as aliquots at -20C. For worm retesting, a 10mM stock was prepared.

High-throughput larval growth assays in worms

The F125L pmm-2 mutant growth screen was conducted in 384-well plates. 320 wells of the plate are filled with 25μM of compound (137.5nL) from the Microsource Spectrum library, dispensed into each well of the plate using an Echo 550 acoustic dispenser from Labcyte, Inc. In addition, all test wells were dispensed with 12.5nL of a 50mM stock of bortezomib solubilized in DMSO, resulting in a final concentration of 11μM. Control wells of the plate were filled with 150nL of DMSO (positive control), or 12.5nL of bortezomib and 137.5nL of DMSO (negative control). Following addition of test compounds, wells were dispensed with 5μL of bacterial media resuspended in S-medium containing cholesterol after adjusting the optical density to 0.45 at 600nm. Mutant animals were grown on standard nematode growth media agar plates until gravid. Adult worms were bleached using hypochlorite treatment to obtain eggs. Eggs were allowed to hatch overnight at 20˚C in order to obtain synchronized L1 larvae. L1 larvae were filtered through 15-micron filters to ensure that the resulting population was clean before sorting. Fifteen L1 larvae are dispensed per well of the 384-well plate using a BioSorter large particle

flow cytometer from Union Biometrica. Plates were sealed and incubated on a shaker at 20˚C for five days. On the fifth day, plates were vortexed and spun down before the addition of 15µL of 8mM sodium azide. The addition of sodium azide immobilized worms after which they were imaged under transmitted light using a custom plate imager. Finally, automated image processing was run on each plate.

Data analysis

We used custom image processing algorithms to extract areas occupied by worms per well. After outlier elimination among controls, i.e., elimination of data points on account of image or experimental artifacts, Z-scores were assigned to each well of the plate relative to the negative controls. Next, all wells that had a Z-score of greater than two in triplicate were isolated and manually inspected. Because bortezomib suppresses larval growth and induces arrest, we determined that a compound rescued the underlying defect if a well had a higher area occupied by worms relative to the negative control. Visual inspection often revealed that in primary screening positive wells, animals attained adulthood and produced progeny.

PMM2 enzymatic assay in worms

L1-stage-synchronized pmm-2 mutant animals were grown (2,000 worms per plate) on NGM agar for 24 hours. After 24 hrs, worms were washed off plates into 15mL conical tubes, washed with filtered autoclaved water, pelleted at 3,200 rpm for 4 mins, and then resuspended in 2mL S-medium. HB101 bacteria grown in LB overnight was pelleted at 4,000 rpm for 10 minutes and resuspended in S-medium with cholesterol to an optical density of 0.35. For each experimental condition, 25mL of HB101 in S-medium was added to 50mL conical tubes along with 15,000 to 20,000 worms. Test compounds were dissolved in DMSO stock solutions and added to samples at a final concentration of 15µM. Samples were incubated at 20˚C for 24 hours. After 24 hours, conical tubes were placed on ice, and worms were allowed to settle for 15 minutes. The bacterial supernatant was aspirated, and the worms were pelleted and washed with water. Worms were transferred to 1.5mL Eppendorf tubes, pelleted at 4˚C, and lysed in 70-100µL homogenization buffer (20mM Hepes, 25mM KCl, 1mM DTT, 10µg/mL leupeptin, 10µg/mL antipain) on ice. The lysate was centrifuged, and 1-2µL of lysate was used for protein quantification using a Qubit. Lysate equivalent of 10µg protein was used per well to determine PMM-2 enzyme activity levels after adding the 200µL of assay buffer. Assay buffer without the

substrate was used as the control and the assay was carried out for 3-4 hours with absorbance readings every 30 minutes at 340nm.

PMM2 enzymatic assay in patient fibroblasts

Briefly, cells were seeded in a 96-well plate, homogenization buffer (20mM Hepes, 25mM KCl, 1mM DTT, 10µg/mL leupeptin, 10µg/mL antipain) was added, and plates were freeze-thawed at -80˚C twice to lyse cells. Reaction buffer containing the substrate was then added to the wells of each plate. Plates were incubated at 37˚C for 30 minutes and absorbance was read at 340nm at regular time points: 30, 60, 90, 120, 150, 180, 210, 240 and 270 minutes. All incubations are carried out with or without substrate (mannose-1-phosphate), and the difference between the two values was taken as the enzymatic activity. Enzyme activity was normalized to total lysate protein levels. Enzyme activity of wildtype fibroblasts and patient-derived compound heterozygous (F119L/R141H) fibroblast line were determined.

To assess if compounds from the phenotypic screens affected enzyme activity, all compounds were incubated with the mutant cell line at a concentration of 10µM for a 24-hour period. Following this, enzyme activity was assessed as described above. At least two biological replicates were conducted and enzyme activity in the presence of a test compound was compared to DMSO-treated mutant cell line. For ease of analysis, we compared the enzyme activity (as represented by NADPH concentration) of each treatment condition to activity of baseline, untreated mutant line at the last time point.

Keap1-NRF2 activation luciferase reporter assay in O2OS cells

Hit compounds were tested by DiscoverX (San Diego) using the PathHunter® eXpress Keap1-NRF2 Nuclear Translocation Assay. Briefly, PathHunter cells are plated and incubated for 24 hours at 37°C. 10µL of test compound was added and cells were incubated with compound for 6 hours at room temperature. Working detection reagent solution was added and plates were incubated for 60 minutes at room temperature. Chemiluminescence signal was read by a SpectraMax M3. Methyl CDDO ester was used as the positive control. To be called a NRF2 activator, a hit compound had a half-maximal effective concentration (EC_{50}) less than 10µM and a slope comparable to methyl CDDO ester.

Quantitative RT-PCR of worms

Worms were age-synchronized and collected as Day-1 adults. Worm pellets were homogenized and RNA extracted following published protocols (Guthmueller et al, 2011). ER stress markers were selected based on the pmm2 zebrafish model (Mukaigasa et al, 2018).

Results

Generation and phenotyping of the first nematode model of PMM2-CDG

The F52B11.6 gene sequence in *C. elegans* is orthologous to human PMM2. Nematode *PMM-2* shares 54% identity with the human protein, and the two most common disease-causing mutations -- R141H and F119L -- are evolutionarily conserved. We first characterized a heterozygous *pmm-2* null strain. This strain has a 518 base pair deletion in the *PMM-2* open reading frame. It is documented to be larval lethal, which we confirmed. The heterozygous animals produce few homozygous null progeny, insufficient for the scale of a high-throughput drug screen. We used quantitative RT-PCR to measure the amount of *PMM-2* mRNA expression in *pmm-2* heterozygote animals. We observed that *PMM-2* mRNA levels are constitutively elevated, indicating that these animals compensate at the transcriptional level to boost *PMM-2* expression to levels normally expressed in wildtype worms with two functional copies of *PMM-2* (**Supplementary Figure 1**). Because *pmm-2* homozygous nulls are inviable and *pmm-2* heterozygous nulls do not exhibit overt phenotypes, we engineered a novel *pmm-2* hypomorphic mutant strain using CRISPR/Cas9. We created a homozygous F125L missense mutant, as F125 is orthologous to human F119. F119 sits in the dimer interface and the F119L mutation results in a defect in dimerization. The homozygous *pmm-2* F125L (hereafter referred to as F119L) strain is homozygous viable and does not exhibit larval lethality, growth defects or any observable locomotor defects in liquid media. We verified that *PMM-2* mRNA transcript levels are comparable to wildtype in the F119L mutant (**Supplementary Figure 1**). In order to determine if the F119L homozygote mutant is a bona fide model of PMM2-CDG, we measured *PMM-2* enzymatic activity in F119L homozygotes after whole-animal lysis. As expected, this mutant has reduced *PMM-2* enzymatic activity, while by contrast *PMM-2* enzymatic activity is unchanged in a *png-1* null mutant and model of NGLY1 Deficiency, another glycosylation disorder, and wildtype (N2) worms (**Figure 1**).

Because the F119L homozygous mutant strain presented no overt differences compared to wildtype worms, it was not amenable to high-throughput screening directly. We asked if *pmm-2*

mutant animals are more sensitive to stressors that disrupt proteasomal processes and induce ER stress. Literature evidence shows that tunicamycin (Buzzi et al, 2011) and bortezomib (Tillman et al, 2018) exposure causes proteasomal stress, activates the unfolded protein response and induces larval arrest in worms. We treated F119L mutant animals with increasing concentrations of tunicamycin and bortezomib. We sought to establish if either compound affected growth and development of mutant animals at concentrations lower than similarly exposed wildtype worms. While tunicamycin did not produce differential larval arrest in mutants and wildtype worms, we found that *pmm-2* mutants exposed to bortezomib, a reversible proteasome inhibitor, displayed larval arrest at concentrations lower than wildtype (**Figure 2B**). Thus, we decided to screen the Microsource Spectrum drug repurposing library in triplicate for compounds that rescue larval arrest in the presence of 11μM bortezomib.

Drug repurposing screen of F119L mutant worms

Representative positive control and negative control wells are shown in **Figure 3**. Statistically significant separation between positive and negative controls allowed us to robustly identify both suppressors and enhancers, which include toxic compounds (**Supplementary Figure 2**). We only examined suppressors in the context of this study, i.e., compounds that suppress the larval arrest induced by 11μM bortezomib. 20 compounds had Z-scores greater than five in all three replicates (**Figure 3A**), resulting in a suppressor hit rate of 0.781% that is consistent with the hit rates we observed in previous whole-organism phenotypic drug repurposing screens in flies (Rodriguez et al, 2018) and yeast (Lao et al, 2019). 12/20 (60%) of the hit compounds are polyphenols: fisetin, gossypetin, rhamnetin, quercetin tetramethyl ether, baicalein, hieracin, epicatechin monogallate, koparin, theaflavin monogallate, ellagic acid, pyrogallin and purpurogallin-4-carboxylic acid. 3/20 (15%) of the hit compounds are the building blocks of more complex polyphenols: 3-methoxycatechol; 2,3,4-trihydroxy-4-methoxybenzophenone; 3,4-didesmethyl-5-deshydroxy-3-ethoxyschleroin. 3/20 (15%) are catecholamines: levodopa, ethylnorepinephrine, and dobutamine. The remaining two chemically simple compounds may be classified as antioxidants: amidol and edavarone. The polyphenol flavonoid 2'-2'-bisepigallocatechin digallate was identified as one of three hits in our yeast PMM2 drug repurposing study (Lao et al, 2019), demonstrating that certain polyphenolic natural products rescue in both yeast and worm species paradigms by a conserved mechanism of action. The structures of representative worm PMM2 repurposing hits are shown in **Figure 4**.

It is known that catechol-containing compounds can directly inactivate bortezomib, resulting in false positive hits (Glynn et al, 2015). We performed several counter-screens in order to prioritize the 20 worm repurposing hits for subsequent testing in PMM2-CDG patient fibroblasts in a PMM2 enzymatic activity assay. These results are summarized in **Table 1**. When we tested all 20 worm repurposing hits on yeast PMM2 models for growth rescue, 10/20 (50%) of the hits improved growth of one or more yeast PMM2 models. When we tested all 20 worm repurposing hits in a NRF2 reporter assay in human cells, 4/20 (20%) of the hits activated NRF2: fisetin, rhamnetin, pyrogallin and purpurogallin-4-carboxylic acid (**Supplementary Figure 3**). Fisetin is a known NRF2 activator (Smirnova et al, 2011). The other three were not previously known to activate NRF2.

Validating hit compounds in PMM2 enzymatic assays in worms and patient fibroblasts

We optimized PMM2 enzymatic assays for worms and for patient fibroblasts based on the previously reported protocol (Van Schaftingen & Jaeken, 1995). We hypothesized that some yeast and worm PMM2 repurposing hits rescue growth defects and developmental delay by potentiating residual PMM2 enzymatic activity. Of the set of three yeast PMM2 repurposing hits reported in Lao *et al* and 20 worm PMM2 repurposing hits, only one compound robustly activated PMM2 enzymatic activity in both worms and fibroblasts: alpha-cyano-4-hydroxycinnamic acid (CHCA). Pyrogallin and fisetin activated PMM2 enzymatic only in fibroblasts. Those two compounds also activate NRF2, indicating a different mechanism of action than CHCA. Based on the results presented here, there are at least three mechanisms of action which correspond to the structural classes of hit compounds that we observed: (1) PMM2 enzyme activation, (2) NRF2 activation, and (3) PMM2 enzyme activation and NRF2 activation.

We focused on CHCA because it had the largest effect size in terms of PMM2 enzymatic activity of all the yeast and worm PMM2 repurposing hits. A literature search reveals that CHCA is an aldose reductase inhibitor (Zhang et al, 2016). Therefore we tested all 14 commercially available aldose reductase inhibitors (ARIs), including those containing a carboxylic acid moiety shared with CHCA. Only epalrestat reproducibly increased PMM2 enzymatic activity in both worms (**Figure 5**) and fibroblasts (**Figure 6**) between 20-40% above baseline. Notably, of the 14 ARIs we tested, only epalrestat is orally bioavailable, brain-penetrant, well-tolerated and approved for use in humans. Epalrestat was approved for the treatment of diabetic neuropathy

in geriatric patients in Japan in 1994 (Hotta et al, 1996), and is also available in China and India, but has not been approved by the Food and Drug Adminstration (FDA) for any indications.

Epalrestat increases PMM2 mRNA expression and rescues ER stress markers in worms

It was recently reported that a *pmm2* hypomorphic mutant zebrafish constitutively activates NRF2 and furthermore that the small molecule NRF2 activator sulforaphane ameliorates endoplasmic reticulum (ER)-associated stress markers (Mukaigasa et al, 2018). Therefore we tested whether epalrestat acts similarly to sulforaphane by interrogating mRNA expression levels of the worm orthologs of the ER stress markers that are induced in a *pmm2* hypomorphic mutant zebrafish. The results of this qPCR analysis are shown in **Figure 7**. *PMM-2* transcript levels are increased by 15μM epalrestat. Transcript levels of *HSP-1*, which encodes a heat shock protein, are also increased by epalrestat treatment. Conversely, the ER stress markers *IRE-1*, *PEK-1*, *SKN-1*, and *GCS-1*, which are constitutively elevated in the F119L mutant, are uniformly decreased by treatment with epalrestat. These results bolster confidence in the translational fidelity of our F119L worm model of PMM2-CDG because it phenocopies a vertebrate model of PMM2-CDG.

Discussion

We set out in this study to build on the results of our previous yeast PMM2 disease modeling and drug repurposing efforts (Lao et al, 2019). We filled a gap in PMM2-CDG disease models by generating a nematode model based on a specific PMM2-CDG mutation, in this case the second-most common missense allele F119L (F125L in worms). We confirmed that the F119L nematode model has between 30-40% residual PMM-2 enzymatic, comparable to the F119L yeast model. We identified increased sensitivity to the proteasome inhibitor bortezomib as a screenable phenotype in an unbiased whole-organism drug repurposing screen. A comparative analysis of yeast and worm PMM2 repurposing hits revealed significant overlap in structural classes, in particular plant-based polyphenols. Using a PMM2 enzymatic activity assay in PMM2-CDG patient fibroblasts, we showed that several overlapping yeast and worm repurposing hits increase PMM2 enzymatic activity. These compounds are the first known small molecule potentiators of PMM2 enzymatic activity. Analysis of structure-activity relationships suggested that at least one class of hit compounds are aldose reductase inhibitors (ARIs). Upon testing all commercially available ARIs, we showed conclusively that epalrestat boosts PMM2 enzymatic activity in both nematodes and human fibroblasts. Epalrestat is the only ARI

approved for use in humans. It's been used to treat peripheral neuropathy in geriatric diabetic patients in Asia for several decades.

What is the mechanism of action by which epalrestat potentiates PMM2 enzymatic activity? We propose here several ways that epalrestat could be increasing PMM2 enzymatic activity. First, activation of NRF2 could lead to increased PMM2 mRNA levels, which in turn would lead to increased PMM2 protein levels. Several reports indicate that epalrestat activates NRF2 in cultured cells (Yama et al, 2016; Yama et al, 2015). We know from our studies of yeast PMM2-CDG models that overexpression of F119L mutant protein can rescue growth defect by mass action effects (Lao et al, 2019). Second, PMM2 enzymatic activity could be potentiated post-translationally by inhibition of the polyol pathway. Aldose reductase inhibitors block the conversion of glucose to sorbitol. Excess of glucose may be shunted toward production of glucose-1,6-bisphosphate, an endogenous small molecule coactivator of PMM2 (Pirard et al, 1999). At the same time, inhibition of the polyol pathway reduces the levels of advanced glycation end products, which would attenuate the sequelae of ER stress and oxidative stress. In humans, epalrestat is known to reduce the levels of carboxymethyl lysine, a known advanced glycation end product (Kawai et al, 2010). Third, there could be complex interaction between activation of NRF2 and inhibition of the polyol pathway, the former acting at the transcriptional level and the latter acting post-translationally.

These models make several testable predictions. First, PMM2 is either a target gene of NRF2 or its expression is increased as an indirect effect of NRF2 activation. Second, the levels of the endogenous PMM2 enzyme coactivator glucose-1,6-bisphosphate are increased by epalrestat. Future studies will elucidate the exact mechanism of action of epalrestat with respect to PMM2 enzyme activation. In the interim, decades of safe and effective administration of epalrestat in geriatric populations for peripheral neuropathy suggests that the drug may also be safe in pediatric settings necessitated by PMM2-CDG. Peripheral neuropathy is observed in almost all PMM2-CDG patients, so a therapeutic rationale for repurposing epalrestat for PMM2-CDG is compelling.

Acknowledgements

We acknowledge Maggie's PMM2-CDG Cure as a funding source, and we thank Dr. Eva Morava for feedback on the manuscript.

Table 1. **Summary of hit compound cross-validation in yeast, worms and fibroblasts**

Compound Name	Worm	Yeast	Fibroblast
pyrogallin	+	-	NRF2 activation and PMM2 enzyme activation
alpha-cyano-4-hydroxycinnamic acid	-	+	PMM2 enzyme activation
purpurogallin-4-carboxylic acid	+	-	NRF2 activation
rhamnetin	+	-	NRF2 activation
fisetin	+	-	NRF2 activation and PMM2 enzyme activation
dobutamine	+	+	unknown
theaflavin monogallate	+	+	unknown
epicatechin monogallate	+	+	unknown
theaflavin digallate	+	+	unknown
ethylnorepinephrine	+	+	unknown
2,3,4'-trihydroxy-4-methoxybenzophenone	+	+	unknown
koparin	+	+	unknown

Figure Legends

Figure 1. Plot of PMM-2 enzymatic activity as measured by production of NADPH concentration (mmol/L) over time. Blue line is wildtype N2 worms. Orange line is COP1626, or the *pmm-2* F125L homozygote mutant. Gray line is GR2246, or a *png-1* deletion mutant.

Figure 2. *pmm-2* F125L homozygote mutant is sensitize to bortezomib. (**A**) Side-by-side comparison of a positive control well containing wildtype worms (left) and a negative control well containing pmm-2 F125L worms treated with 13.6μM bortezomib. (**B**) Box plot dose-response curve of *pmm-2* F125L worms treated with a range of concentrations of bortezomib.

Figure 3. Summary of drug repurposing screen of pmm-2 F125L mutant worms. (**A**) Three replicates of the Microsource Spectrum library screen (replicate 1 = gray circles, replicate 2 = gray squares, replicate 3 = gray triangles). Black circles represent the 20 hit compounds with Z-scores greater than five in all three replicates. Each column represents one of the eight library plates. The lower black line indicates Z-score = 0. The upper black line indicates Z-score = 5. (**B**) Representative positive control well. (**C**) Representative negative control well. (**D**) Representative suppressor (hit) well. (**E**) Representative enhancer/toxic well.

Figure 4. Chemical structures of worm PMM2 repurposing hits. (**1**) fisetin. (**2**) quercetin tetramethylether. (**3**) gossypetin. (**4**) rhamnetin. (**5**) baicalein. (**6**) epicatechin monogallate. (**7**) theaflavin monogallate. (**8**) pyrogallin. (**9**) ellagic acid. (**10**) levodopa. (**11**) ethyl norepinephrine. (**12**) dobutamine.

Figure 5. PMM-2 enzymatic activity assay of PMM2-CDG worm model. X-axis is NADPH concentration expressed as a percentage of the baseline pmm-2 F125L mutant. From left to right: pmm-2 F125L (F119L) homozygote mutant treated with DMSO vehicle; pmm-2 F125L (F119L) homozygote mutant treated with 15μM epalrestat; pmm-2 F125L (F119L) homozygote mutant treated with 15μM alpha-cyano-4-hydroxycinnamic acid. Error bars represent standard error.

Figure 6. PMM2 enzymatic activity assay of PMM2-CDG patient fibroblast. X-axis is NADPH concentration over time. Orange line is the pmm-2 F125L (F119L) homozygote mutant baseline PMM-2 enzymatic activity. Gray line is the pmm-2 F125L (F119L) homozygote mutant treated with 10μM epalrestat for 24 hours.

Figure 7. Quantitative RT-PCR analysis of PMM-2 and ER stress marker expression in pmm-2 F125L (F119L) homozygote mutant worms.

Supplemental Figure 1. Quantitative RT-PCR analysis of PMM-2 expression in pmm-2 F125L (F119L) homozygote mutant worms compared to the heterozygous *pmm-2* deletion mutant.

Supplemental Figure 2. Box plots of positive and negative control wells from a representative replicate of the Microsource Spectrum drug repurposing library screen.

Supplemental Figure 3. Dose-response curves of four worm PMM2 repurposing hits in a Keap1-NRF2 reporter activation assay in human cells generated by DiscoverX. (**A**) pyrogallin. (**B**) fisetin. (**C**) rhamnetin. (**D**) purpurogallin-4-carboxylic acid.

References

Andreotti, G., Monti, M.C., Citro, V. & Cubellis, M.V. (2015). Heterodimerization of Two Pathological Mutants Enhances the Activity of Human Phosphomannomutase2. PLos One, 10(10), e0139882.

Buzzi, L.I., Simonetta, S.H., Parodi, A.J. & Castro OA. (2011). The two Caenorhabditis elegans UDP-glucose:glycoprotein glucosyltransferase homologues have distinct biological functions. PLoS One, 6(11), e27025.

Cabezas, O.R., Flanagan, S.E., Stanescu, H., García-Martínez, E., Caswell, R., Lango-Allen, H., Antón-Gamero, M., Argente, J., Bussell, A.M., Brandli, A., Cheshire, C., Crowne, E., Dumitriu, S., Drynda, R., Hamilton-Shield, J.P., Hayes, W., Hofherr, A., Iancu, D., Issler, N., Jefferies, C., Jones, P., Johnson, M., Kesselheim, A., Klootwijk, E., Koettgen, M., Lewis, W., Martos, J.M., Mozere, M., Norman, J., Patel, V., Parrish, A., Pérez-Cerdá, C., Pozo, J., Rahman, S.A., Sebire, N., Tekman, M., Turnpenny, P.D., Hoff, W.V., Viering, D.H.H.M., Weedon, M.N., Wilson, P., Guay-Woodford, L., Kleta, R., Hussain, K., Ellard, S., Bockenhauer, D. (2017). Polycystic Kidney Disease with Hyperinsulinemic Hypoglycemia Caused by a Promoter Mutation in Phosphomannomutase 2. Journal of the American Society of Nephrology, 28(8), 2529-2539.

Chang, I.J., He, M. & Lam CT. (2018). Congenital disorders of glycosylation. Annals of Translational Medicine, 6(24), 477.

Citro, V., Cimmaruta, C., Monticelli, M., Riccio, G., Hay Mele, B., Cubellis, M.V. & Andreotti G. (2018). The Analysis of Variants in the General Population Reveals That PMM2 Is Extremely Tolerant to Missense Mutations and That Diagnosis of PMM2-CDG Can Benefit from the Identification of Modifiers. International Journal of Molecular Sciences, 19(8), 2218.

Cline, A., Gao, N., Flanagan-Steet, H., Sharma, V., Rosa, S., Sonon, R., Azadi, P., Sadler, K.C., Freeze, H.H., Lehrman, M.A. & Steet R. (2012). A zebrafish model of PMM2-CDG reveals altered neurogenesis and a substrate-accumulation mechanism for N-linked glycosylation deficiency. Molecular Biology of the Cell, 23(21), 4175-4187.

Glynn, S.J., Gaffney, K.J., Sainz, M.A., Louie, S.G. & Petasis, N.A. (2015). Molecular characterization of the boron adducts of the proteasome inhibitor bortezomib with epigallocatechin-3-gallate and related polyphenols. Organic & Biomolecular Chemistry, 13(13), 3887-3899.

Guthmueller, K.L., Yoder, M.L. & Holgado, A.M. (2011). Determining Genetic Expression Profiles in C. elegans Using Microarray and Real-time PCR. JoVE, 53, 2777.

Hotta, N., Sakamoto, N., Shigeta, Y., Kikkawa, R. & Goto Y. (1996). Clinical investigation of epalrestat, an aldose reductase inhibitor, on diabetic neuropathy in Japan: multicenter study. Diabetic Neuropathy Study Group in Japan. Journal of Diabetes Complications, 10(3), 1996.

Hotta, N., Akanuma, Y., Kawamori, R., Matsuoka, K., Oka, Y., Shichiri, M., Toyota, T., Nakashima, M., Yoshimura, I., Sakamoto, N. & Shigeta, Y. (2006). Long-term clinical effects of epalrestat, an aldose reductase inhibitor, on diabetic peripheral neuropathy: the 3-year, multicenter, comparative Aldose Reductase Inhibitor-Diabetes Complications Trial. Diabetes Care, 29(7), 1538-1544.

Izquierdo-Serra, M., Martínez-Monseny, A.F., López, L., Carrillo-García, J., Edo, A., Ortigoza-Escobar, J.D., García, Ó., Cancho-Candela, R., Carrasco-Marina, M.L.,

Gutiérrez-Solana, L.G., Cuadras, D., Muchart, J., Montero, R., Artuch, R., Pérez-Cerdá, C., Pérez, B., Pérez-Dueñas, B., Macaya, A., Fernández-Fernández, J.M. & Serrano M. (2018). Stroke-Like Episodes and Cerebellar Syndrome in Phosphomannomutase Deficiency (PMM2-CDG): Evidence for Hypoglycosylation-Driven Channelopathy. International Journal for Molecular Sciences, 19(2), 619.

Jaeken, J., Vanderschueren-Lodeweyckx, M., Casaer, P., Snoeck, L., Corbeel, L., Eggermont, E. & Eeckels, R. (1980). Familial psychomotor retardation with markedly fluctuating serum prolactin, FSH and GH levels, partial TBG-deficiency, increased serum arylsulphatase A and increased CSF protein: a new syndrome? Pediatric Research, 14, 179.

Kawai, T., Takei, I., Tokui, M., Funae, O., Miyamoto, K., Tabata, M., Hirata, T., Saruta, T., Shimada, A. & Itoh H. (2010). Effects of epalrestat, an aldose reductase inhibitor, on diabetic peripheral neuropathy in patients with type 2 diabetes, in relation to suppression of N(ε)-carboxymethyl lysine. Journal of Diabetes Complications, 24(6), 424-432.

Kjaergaard, S., Skovby, F. & Schwartz, M. (1998). Absence of homozygosity for predominant mutations in PMM2 in Danish patients with carbohydrate-deficient glycoprotein syndrome type 1. European Journal of Human Genetics, 6(4), 331-336.

Lao, J.P., DiPrimio, N., Prangley, M., Sam, F.S., Mast, J.D. & Perlstein EO. (2019). Yeast models of phosphomannomutase 2 deficiency, a congenital disorder of glycosylation. G3, 9(2), 413-423.

Matthijs, G., Schollen. E., Pardon, E., Veiga-Da-Cunha, M., Jaeken, J., Cassiman, J.J. & Van Schaftingen, E. (1997). Mutations in PMM2, a phosphomannomutase gene on chromosome 16p13, in carbohydrate-deficient glycoprotein type I syndrome (Jaeken syndrome). Nature Genetics, 16(1), 88-92.

Matthijs, G., Schollen, E., Van Schaftingen, E., Cassiman, J.J. & Jaeken J. (1998). Lack of homozygotes for the most frequent disease allele in carbohydrate-deficient glycoprotein syndrome type 1A. American Journal of Human Genetics, 62(3), 542-550.

Monin, M.L., Mignot, C., De Lonlay, P., Héron, B., Masurel, A., Mathieu-Dramard, M., Lenaerts, C., Thauvin, C., Gérard, M., Roze, E., Jacquette, A., Charles, P., de Baracé, C., Drouin-Garraud, V., Khau Van Kien, P., Cormier-Daire, V., Mayer, M., Ogier, H., Brice, A., Seta, N &, Héron D. (2014). 29 French adult patients with PMM2-congenital disorder of glycosylation: outcome of the classical pediatric phenotype and depiction of a late-onset phenotype. Orphanet Journal of Rare Diseases, 9, 207.

Mukaigasa, K., Tsujita, T., Nguyen, V.T., Li, L., Yagi, H., Fuse, Y., Nakajima-Takagi, Y., Kato, K., Yamamoto, M. & Kobayashi M. (2018). Nrf2 activation attenuates genetic endoplasmic reticulum stress induced by a mutation in the phosphomannomutase 2 gene in zebrafish. PNAS, 115(11), 2758-2763.

Parkinson, W.M., Dookwah, M., Dear, M.L., Gatto, C.L., Aoki, K., Tiemeyer, M. & Broadie, K. (2016). Synaptic roles for phosphomannomutase type 2 in a new Drosophila congenital disorder of glycosylation disease model. Disease Models and Mechanisms, 9(5), 513-527.

Pirard, M., Achouri, Y., Collet, J.F., Schollen, E., Matthijs, G. & Van Schaftingen E. (1999). Kinetic properties and tissular distribution of mammalian phosphomannomutase isozymes. Biochemistry Journal, 339, 201-207.

Rodriguez, T.P., Mast, J.D., Hartl, T., Lee, T., Sand, P. & Perlstein, E.O. (2018). Defects in the Neuroendocrine Axis Contribute to Global Development Delay in a Drosophila Model of NGLY1 Deficiency. G3, 8(7), 2193-2204.

Smirnova, N.A., Haskew-Layton, R.E., Basso, M., Hushpulian, D.M., Payappilly, J.B., Speer, R.E., Ahn, Y.H., Rakhman, I., Cole, P.A., Pinto, J.T., Ratan, R.R. & Gazaryan, I.G. (2011). Development of Neh2-luciferase reporter and its application for high throughput screening and real-time monitoring of Nrf2 activators. Chemisty & Biology, 18(6), 752-765.

Tillman, E.J., Richardson, C.E., Cattie, D.J., Reddy, K.C., Lehrbach, N.J., Droste, R., Ruvkun, G. & Kim DH. (2018). Endoplasmic Reticulum Homeostasis Is Modulated by the Forkhead Transcription Factor FKH-9 During Infection of Caenorhabditis elegans. Genetics, 210(4), 1329-1337.

Van Schaftingen, E. & Jaeken, J. (1995). Phosphomannomutase deficiency is a cause of carbohydrate-deficient glycoprotein syndrome type I. FEBS Letters, 377(3), 318-320.

Yama, K., Sato, K., Murao, Y., Tatsunami, R. & Tampo Y. (2016). Epalrestat Upregulates Heme Oxygenase-1, Superoxide Dismutase, and Catalase in Cells of the Nervous System. Biological & Pharmaceutical Bulletin, 39(9), 1523-1530.

Yama, K., Sato, K., Abe, N., Murao, Y., Tatsunami, R. & Tampo Y. (2015). Epalrestat increases glutathione, thioredoxin, and heme oxygenase-1 by stimulating Nrf2 pathway in endothelial cells. Redox Biology, 4, 87-96.

Yuste-Checa, P., Gámez, A., Brasil, S., Desviat, L.R., Ugarte, M., Pérez-Cerdá, C. & Pérez, B. (2015). The effects of PMM2-CDG-causing mutations on the folding, activity, and stability of the PMM2 protein. Human Mutations, 36(9), 851-860.

Yuste-Checa, P., Brasil, S., Gámez, A., Underhaug, J., Desviat, L.R., Ugarte, M., Pérez-Cerdá, C., Martinez, A. & Pérez, B. (2017). Pharmacological Chaperoning: A Potential Treatment for PMM2-CDG. Human Mutations, 38(2), 160-168.

Zhang, L., Li, Y.F., Yuan, S., Zhang, S., Zheng, H., Liu, J., Sun, P., Gu, Y., Kurihara, H., He, R.R. & Chen, H. (2016). Bioactivity Focus of α-Cyano-4-hydroxycinnamic acid (CHCA) Leads to Effective Multifunctional Aldose Reductase Inhibitors. Scientific Reports, 6, 24942.

Figure 1

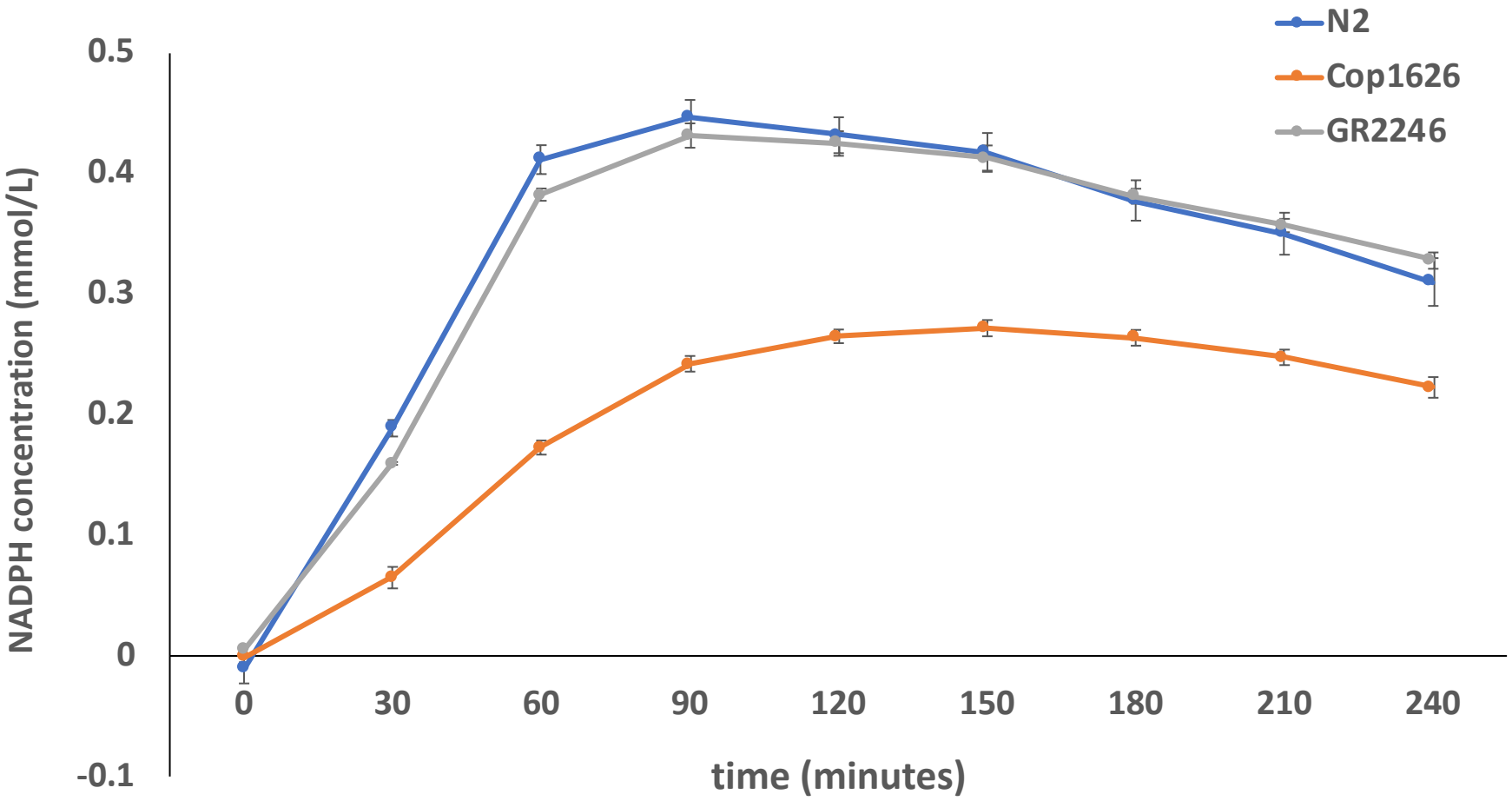
N2
Cop1626
GR2246
0.5
0.4
0.3
0.2
0.1
0
-0.1
NADPH concentration (mmol/L)
0
30
60
90
120
150
180
210
240
time (minutes)

Figure 2

A

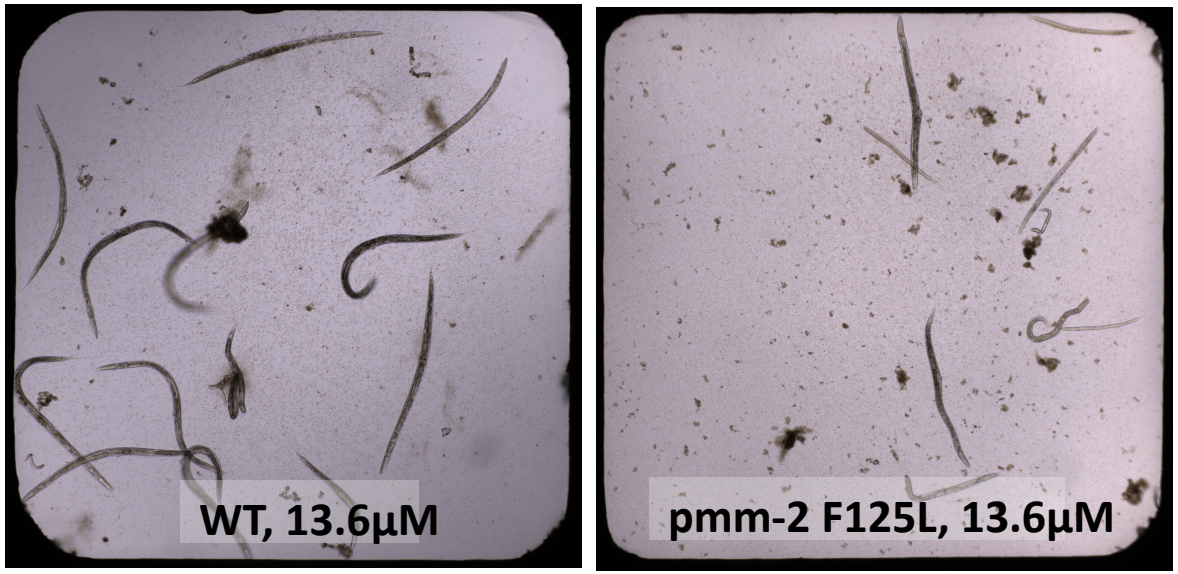
WT, 13.6µM
pmm-2 F125L, 13.6µM

B

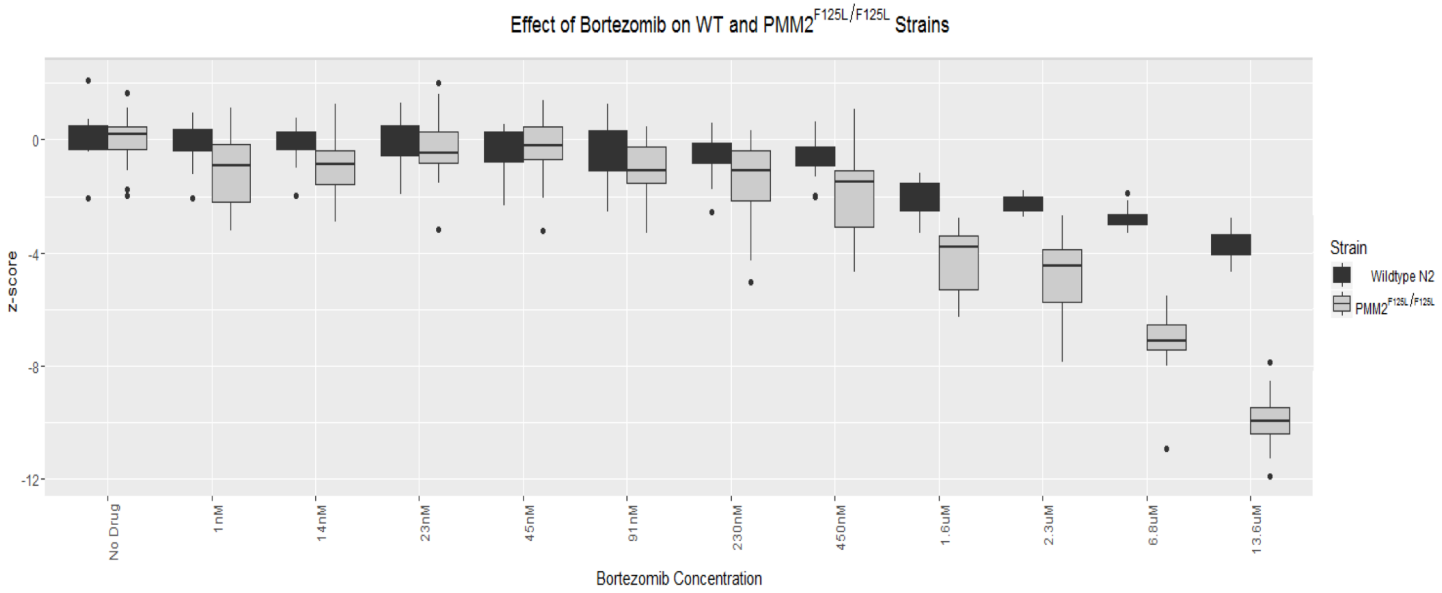
Effect of Bortezomib on WT and PMM2F125L/F125L Strains
z-score
0
-4
-8
-12
No Drug
1nM
14nM
23nM
45nM
91nM
230nM
450nM
1.6uM
2.3uM
6.8uM
13.6uM
Bortezomib Concentration
Strain
Wildtype N2
PMM2F125L/F125L

Figure 3

A

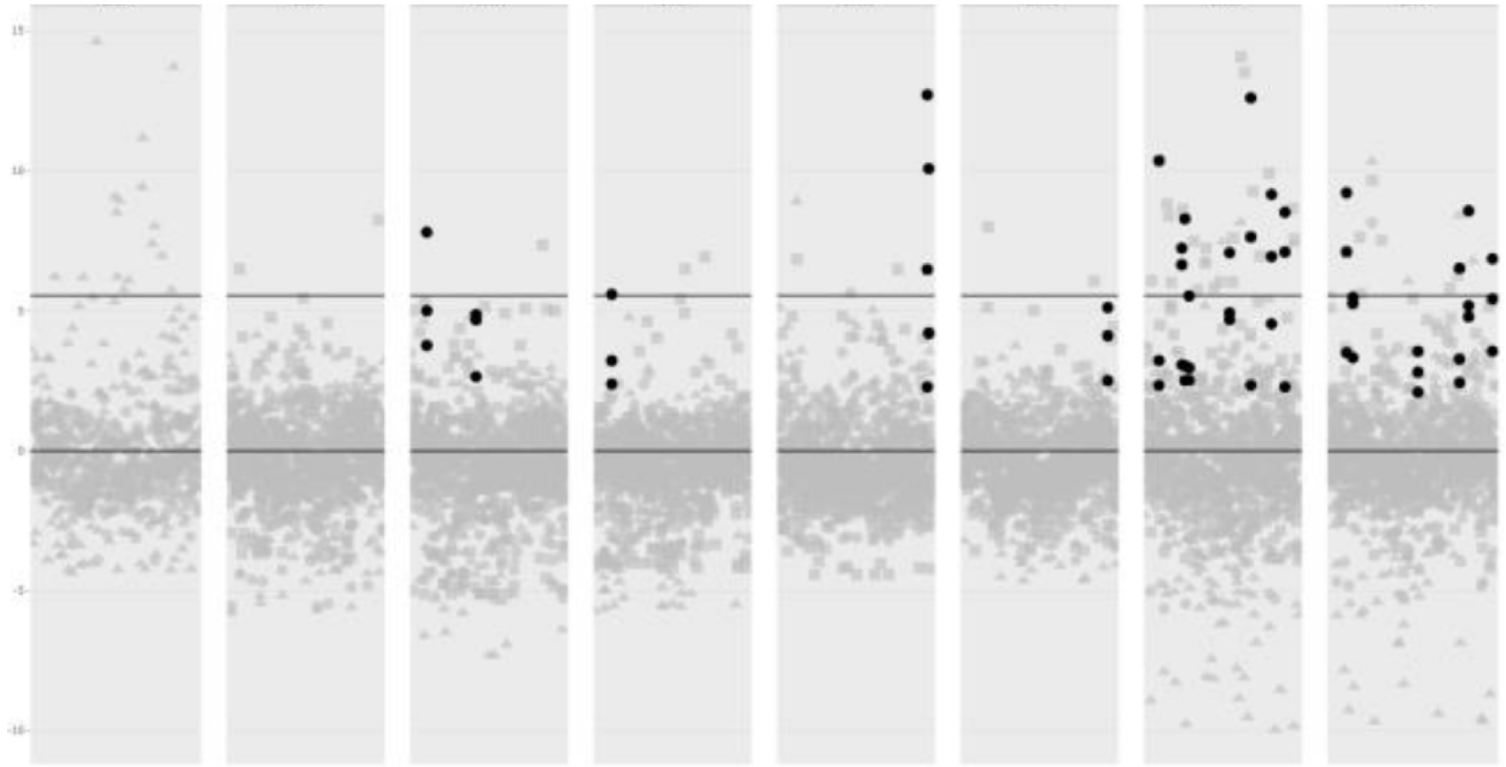

B

C

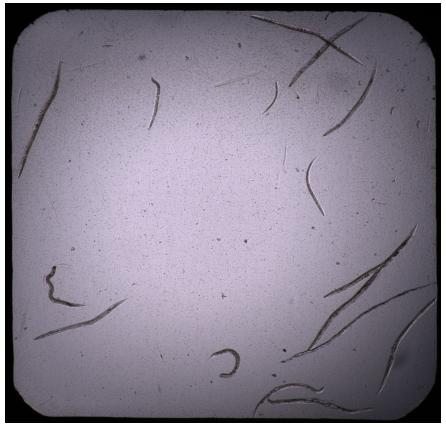

D

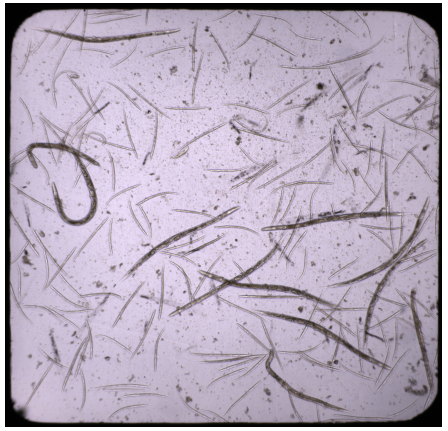

E

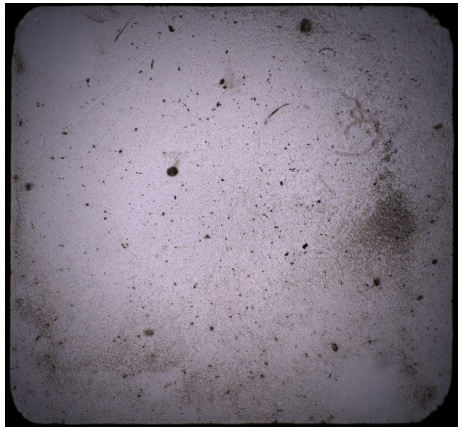

Figure 4

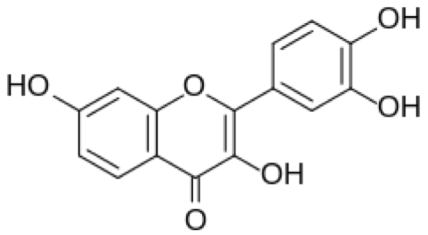

1

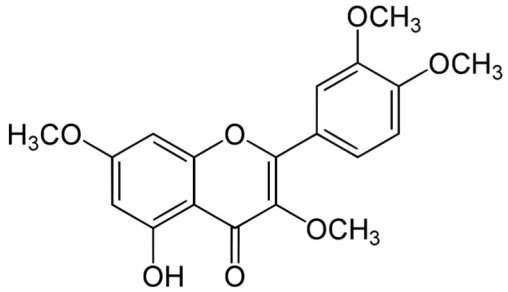

2

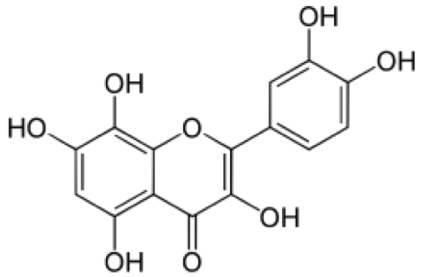

3

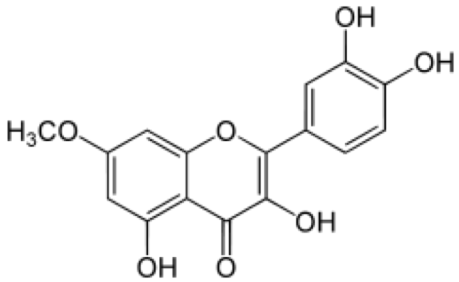

4

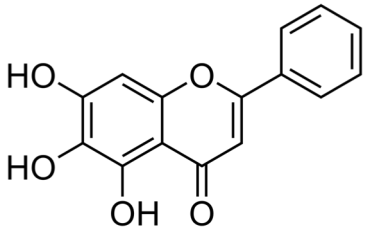

5

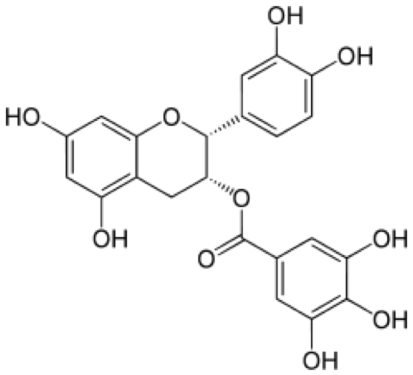

6

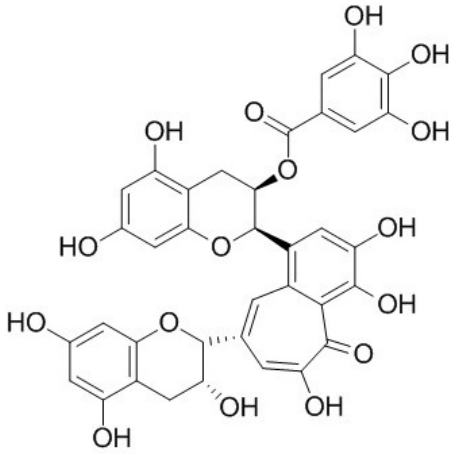

7

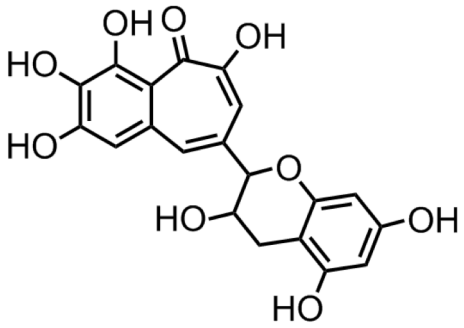

8

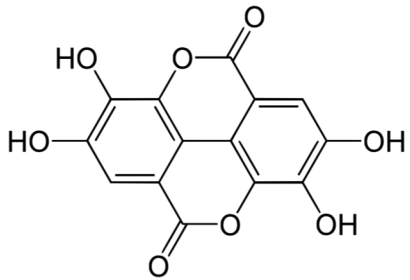

9

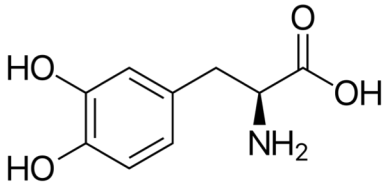

10

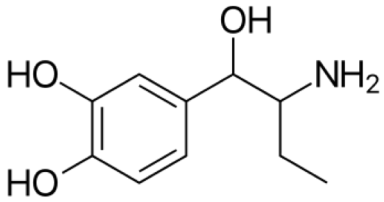

11

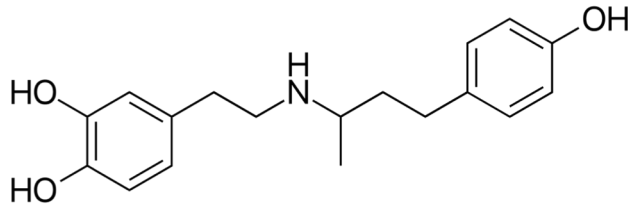

12

Figure 5

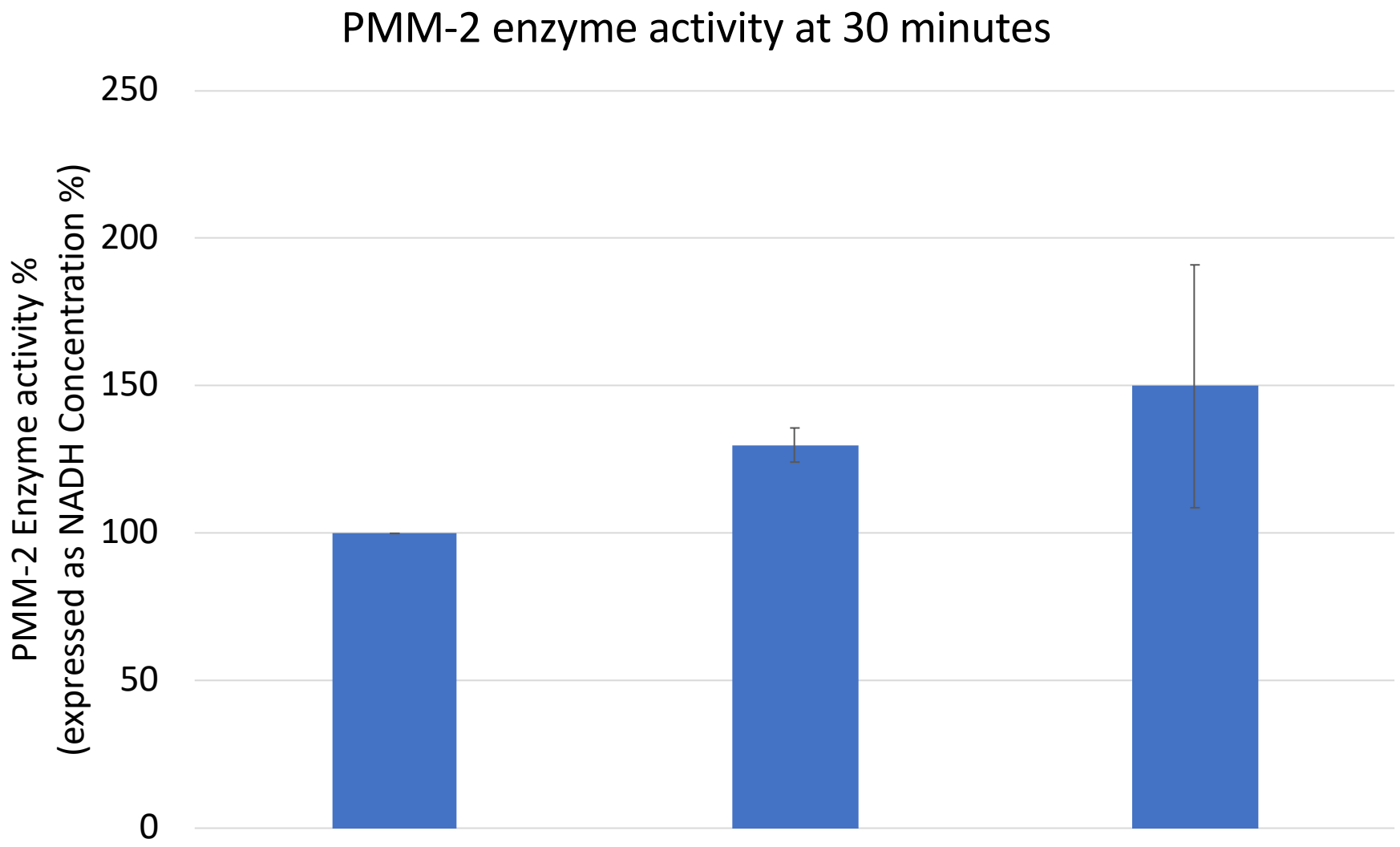
PMM-2 enzyme activity at 30 minutes
PMM-2 Enzyme activity %
(expressed as NADH Concentration %)
250
200
150
100
50
0

Figure 6

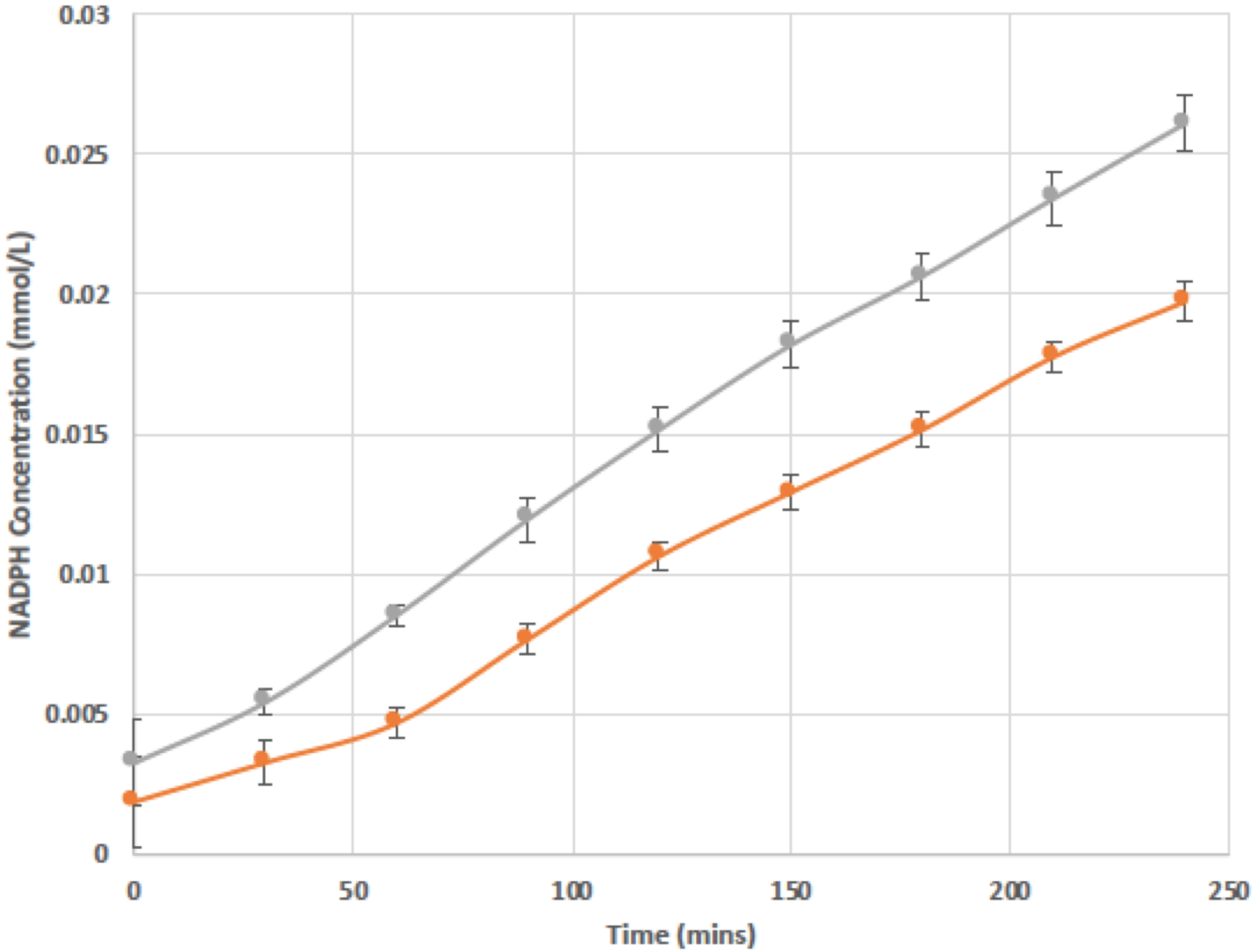
0.03
0.025
0.02
0.015
0.01
0.005
0
NADPH Concentration (mmol/L)
0
50
100
150
200
250
Time (mins)

Figure 7

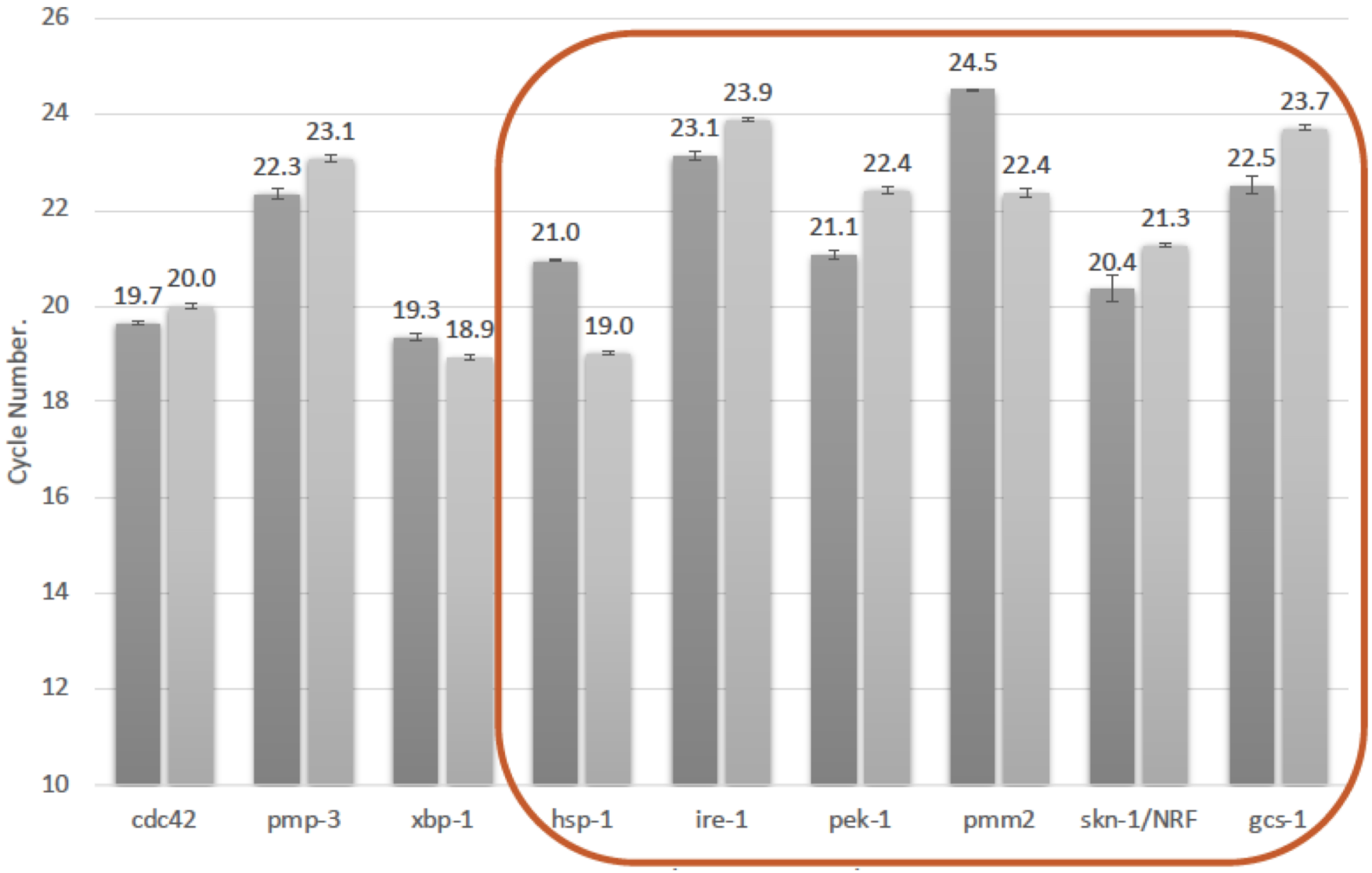
Cycle Number.
26
24
22
20
18
16
14
12
10
19.7
20.0
22.3
23.1
19.3
18.9
21.0
19.0
23.1
23.9
21.1
22.4
24.5
22.4
20.4
21.3
22.5
23.7
cdc42
pmp-3
xbp-1
hsp-1
ire-1
pek-1
pmm2
skn-1/NRF
gcs-1

Supplementary Figure 1

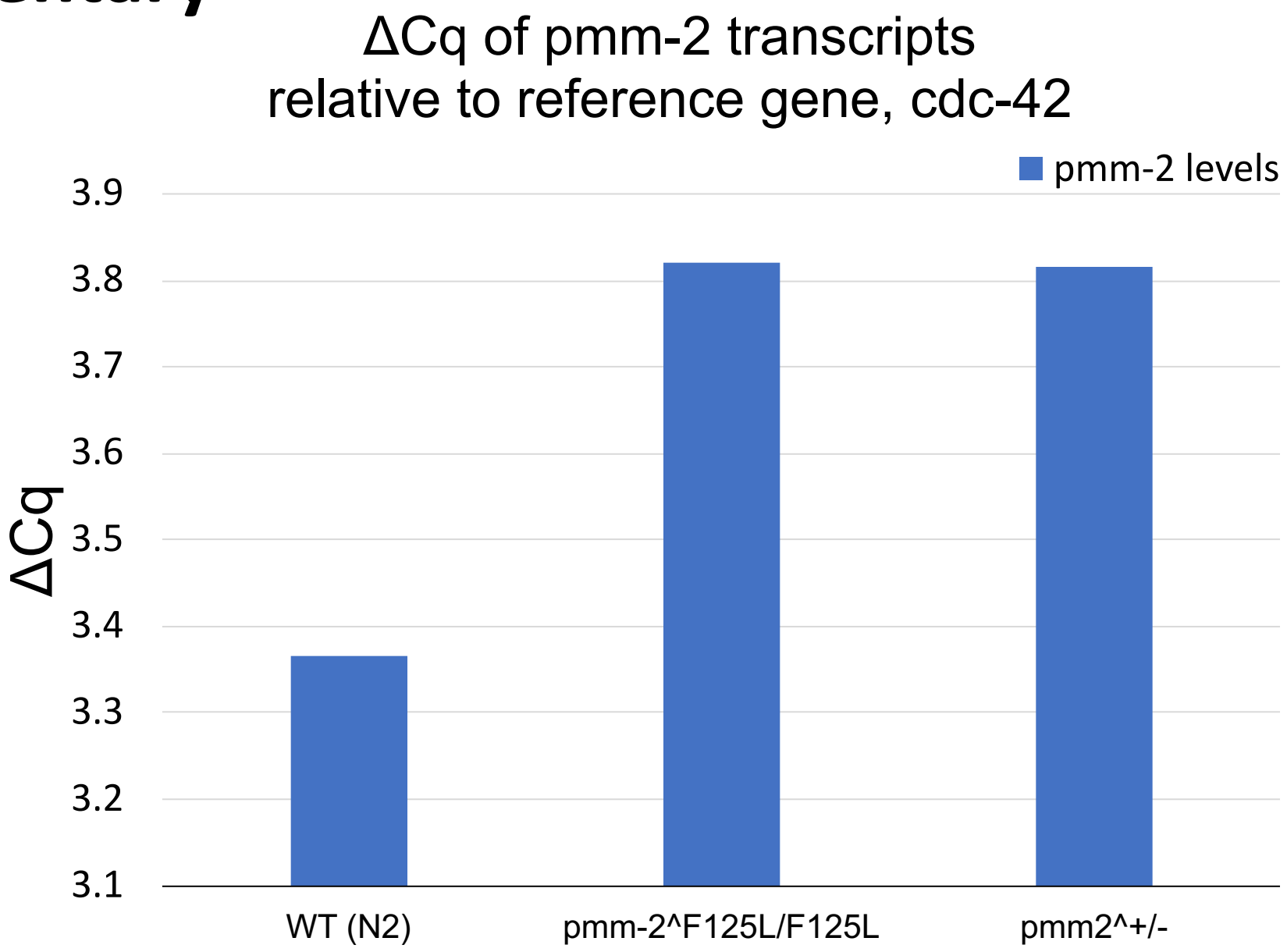

Supplementary Figure 2

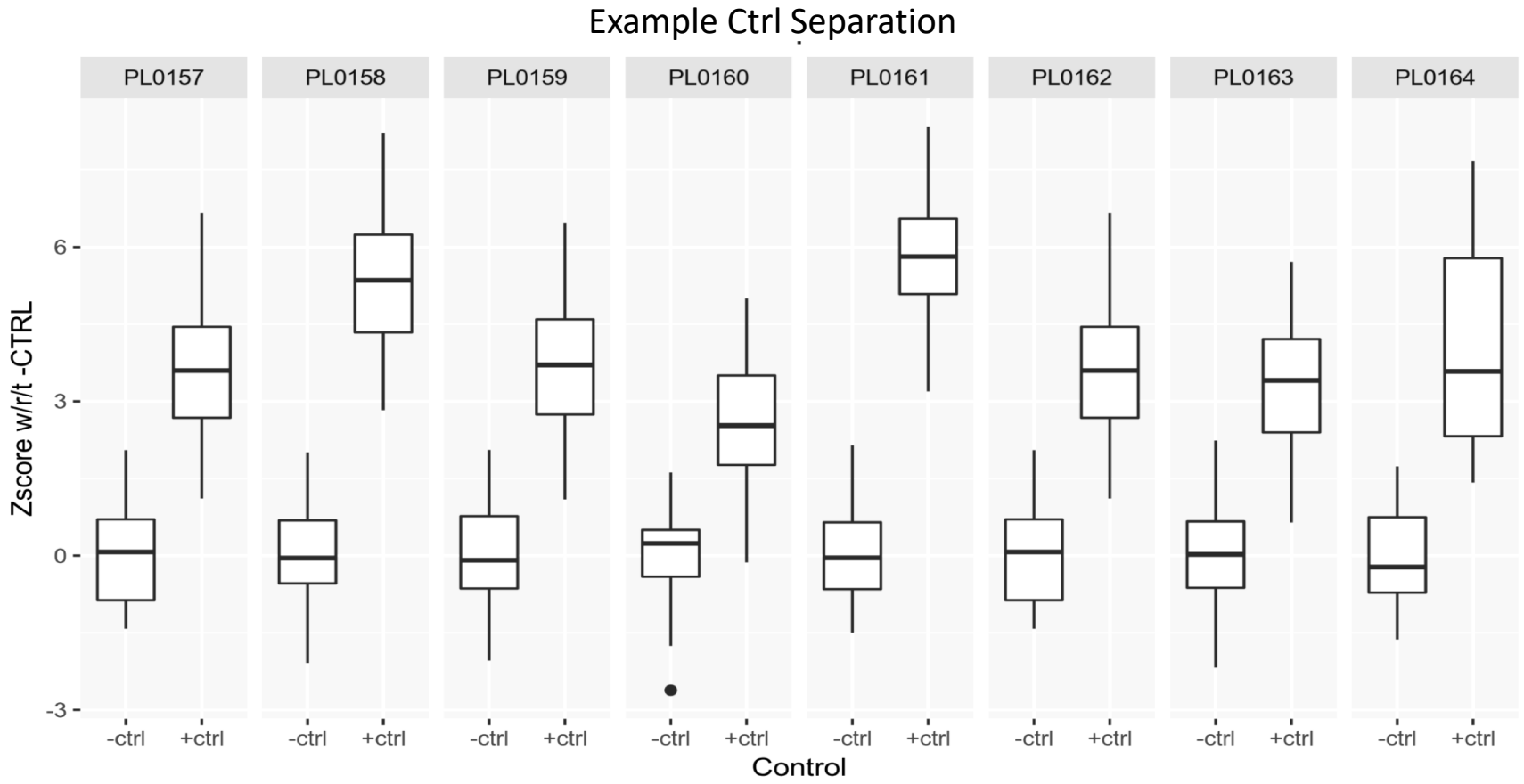

Supplementary Figure 3